


See discussions, stats, and author profiles for this publication at: <https://www.researchgate.net/publication/239671033>

# Noncovalent Synthesis of Nanostructures: Combining Coordination Chemistry and Hydrogen Bonding

**ARTICLE** in ANGEWANDTE CHEMIE INTERNATIONAL EDITION IN ENGLISH · MAY 1997  
Impact Factor: 13.45 · DOI: 10.1002/anie.199710061

CITATIONS  
112


5 AUTHORS, INCLUDING:



[Wilhelm Huck](#)  
Radboud University Nijmegen  
250 PUBLICATIONS 13,478 CITATIONS

SEE PROFILE

READS  
26



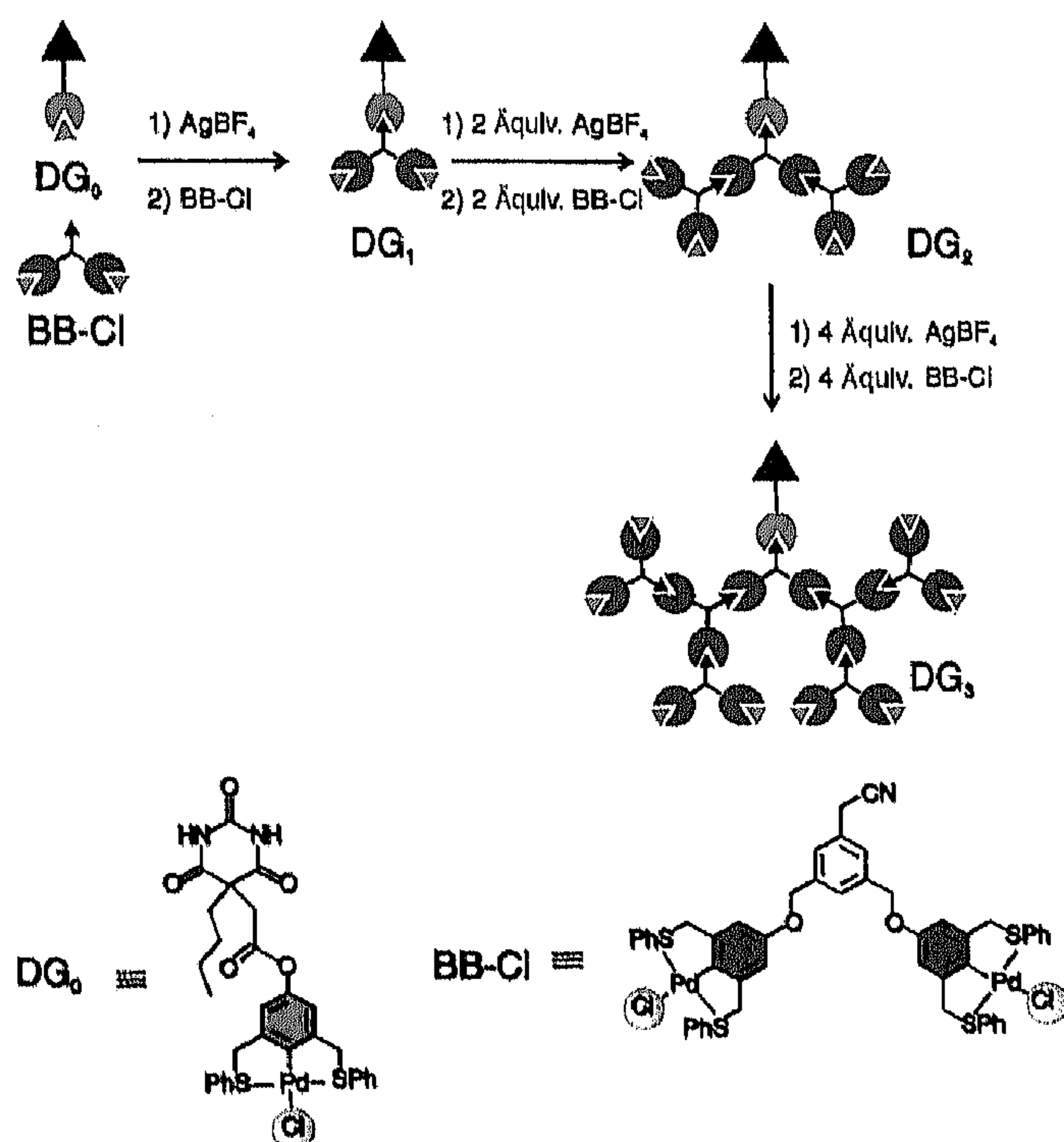
[Peter Timmerman](#)  
University of Amsterdam  
97 PUBLICATIONS 4,287 CITATIONS

SEE PROFILE

# Noncovalent Synthesis of Nanostructures: Combining Coordination Chemistry and Hydrogen Bonding\*\*

Wilhelm T. S. Huck, Ron Hulst, Peter Timmerman,  
Frank C. J. M. van Veggel,\* and David N. Reinhoudt\*

For the synthesis of nanosized particles with structures defined at the molecular level, conventional methods of multistep covalent synthesis have reached their limitations. Consequently, noncovalent synthetic methodologies that equal the precision of covalent synthesis but proceed by simple assembly of building blocks are needed. Such methods should be self-correcting under conditions of thermodynamic equilibrium. Zimmerman et al.<sup>[1]</sup> have exploited hydrogen bonding in the self-assembly of dendrimers centered around a hydrogen-bonded, hexameric nucleus, and we have described a divergent assembly route to dendrimers using coordination chemistry.<sup>[2,3]</sup> Hitherto, the combination of two different types of compatible, noncovalent interactions for the assembly of finite nanostructures has not been employed.<sup>[4]</sup> Here we describe the combined use of hydrogen bonding and coordination chemistry in the assembly of nanosized metallodendrimers with molecular weights of up to 28 kDa. The combination of three metallodendrimer wedges, constructed by coordination chemistry, into a hydrogen-bonded rosette<sup>[5,6]</sup> allows fast and controlled assembly of nanostructures by both divergent<sup>[7]</sup> and convergent<sup>[8]</sup> strategies.



Scheme 1. Controlled assembly of rosette dendrons.

[\*] Dr. Ir. F. C. J. M. van Veggel, Prof. Dr. Ir. D. N. Reinhoudt, Drs. W. T. S. Huck, Dr. P. Timmerman  
Laboratory of Supramolecular Chemistry and Technology and  
MESA Research Institute  
Dr. R. Hulst  
Laboratory of Chemical Analysis  
University of Twente  
P. O. Box 217, NL-7500 AE Enschede (The Netherlands)  
Fax: Int. code + (53) 489-4645  
e-mail: smeta@ct.utwente.nl

[\*\*] We thank the Dutch Foundation for Chemical Research (SON) for financial support.

Dendrons DG<sub>0</sub><sup>[9,10]</sup> to DG<sub>3</sub> (Scheme 1), which contain one barbituric acid residue capable of hydrogen bonding, were synthesized on a 50 mg scale by controlled assembly of appropriate building blocks. DG<sub>1</sub> was assembled from DG<sub>0</sub> by activating the Pd center with AgBF<sub>4</sub>. This gives an intermediate, cationic solvento complex, to which the bis(Pd–Cl) building block BB–Cl<sup>[3]</sup> coordinates (through its cyano moiety). The higher generation dendrons DG<sub>2</sub> and DG<sub>3</sub> were assembled in a one-pot procedure by repeating these activation and addition steps.

The activation by AgBF<sub>4</sub> and the assembly of the building blocks are fast and quantitative reactions; purification is not necessary, and precipitated AgCl is easily removed by filtration. DG<sub>1</sub>–DG<sub>3</sub> were characterized by <sup>1</sup>H NMR spectroscopy, ES-MS (ES = electrospray), and elemental analysis (Table 1).<sup>[11]</sup> In

Table 1. Selected physical data for DG<sub>0</sub>–DG<sub>3</sub>.

DG<sub>0</sub>: M.p. 143–144 °C; <sup>1</sup>H NMR (250 MHz, CDCl<sub>3</sub>, 25 °C, TMS): δ = 8.40 (s, 2H, NH), 7.81–7.75 (m, 4H, Ar<sub>S</sub>H), 7.42–7.23 (m, 6H, Ar<sub>S</sub>H), 6.83 (s, 2H, Ar<sub>Pd</sub>H), 4.53 (br. s, 4H, CH<sub>2</sub>S), 3.40 (s, 2H, C(O)CH<sub>2</sub>), 1.92–1.88 (m, 2H, CH<sub>2</sub>), 1.6 (br. s, 2H, H<sub>2</sub>O), 1.31–1.25 (m, 4H, CH<sub>2</sub>), 0.87 (t, 3H, CH<sub>3</sub>); <sup>13</sup>C NMR (CDCl<sub>3</sub>): δ = 171.7, 150.4, 147.6, 132.0, 131.5, 130.3, 129.8, 115.2, 53.0, 51.6, 40.1, 38.8, 26.1, 22.4, 13.6; FAB-MS (*m*-nitrobenzyl alcohol, NBA): *m/z* = 669.2 ([*M* – Cl]<sup>+</sup>), calcd 667.9; elemental analysis calcd for C<sub>30</sub>H<sub>29</sub>O<sub>5</sub>S<sub>2</sub>N<sub>2</sub>PdCl·H<sub>2</sub>O: C 49.94, H 4.33, N 3.88; found: C 50.34, H 4.28, N 3.76.

DG<sub>1</sub>: M.p. 146–147 °C; <sup>1</sup>H NMR (250 MHz, CD<sub>3</sub>NO<sub>2</sub>, 25 °C, TMS): δ = 8.77 (s, 2H, NH), 7.79–7.73 (m, 12H, Ar<sub>S</sub>H), 7.50 (s, 2H, ArH), 7.38–7.30 (m, 19H, Ar<sub>S</sub>H, ArH), 6.68 (s, 6H, Ar<sub>Pd</sub>H), 5.06 (s, 4H, CH<sub>2</sub>O), 4.6 (br. s, 12H, CH<sub>2</sub>S), 3.94 (s, 2H, CH<sub>2</sub>CN), 3.39 (s, 2H, C(O)CH<sub>2</sub>), 1.96–1.93 (m, 2H, CH<sub>2</sub>), 1.35–1.31 (m, 4H, CH<sub>2</sub>), 0.90 (t, 3H, CH<sub>3</sub>); ES-MS: *m/z* = 1765.0 ([*M* – BF<sub>4</sub>]<sup>+</sup>), calcd 1766.4; elemental analysis calcd for C<sub>80</sub>H<sub>70</sub>O<sub>5</sub>S<sub>6</sub>N<sub>3</sub>Pd<sub>3</sub>Cl<sub>2</sub>BF<sub>4</sub>·2H<sub>2</sub>O: C 50.82, H 3.94, N 2.22, S 10.17, Cl 3.76; found: C 50.61, H 3.92, N 2.40, S 9.64, Cl 4.06.

DG<sub>2</sub>: M.p. 149–150 °C; <sup>1</sup>H NMR (250 MHz, CD<sub>3</sub>NO<sub>2</sub>, 25 °C, TMS): δ = 8.54 (s, 2H, NH), 7.69–7.64 (m, 28H, Ar<sub>S</sub>H), 7.39 (s, 6H, ArH), 7.33–7.28 (m, 45H, Ar<sub>S</sub>H, ArH), 6.67 (s, 14H, Ar<sub>Pd</sub>H), 4.98 (s, 12H, CH<sub>2</sub>O), 4.5 (br. s, 28H, CH<sub>2</sub>S), 3.81 (s, 6H, CH<sub>2</sub>CN), 3.27 (s, 2H, C(O)CH<sub>2</sub>), 1.95–1.91 (m, 2H, CH<sub>2</sub>), 1.35–1.32 (m, 4H, CH<sub>2</sub>), 0.80 (t, 3H, CH<sub>3</sub>); ES-MS: *m/z* = 3986.0 ([*M* – 2BF<sub>4</sub>]<sup>+</sup>), calcd 3983.2; elemental analysis calcd for C<sub>180</sub>H<sub>152</sub>O<sub>11</sub>S<sub>14</sub>N<sub>5</sub>Pd<sub>7</sub>Cl<sub>4</sub>B<sub>3</sub>F<sub>12</sub>: C 52.01, H 3.69, N 1.68, S 10.80, Cl 3.41; found: C 52.24, H 3.84, N 1.66, S 10.63, Cl 3.32.

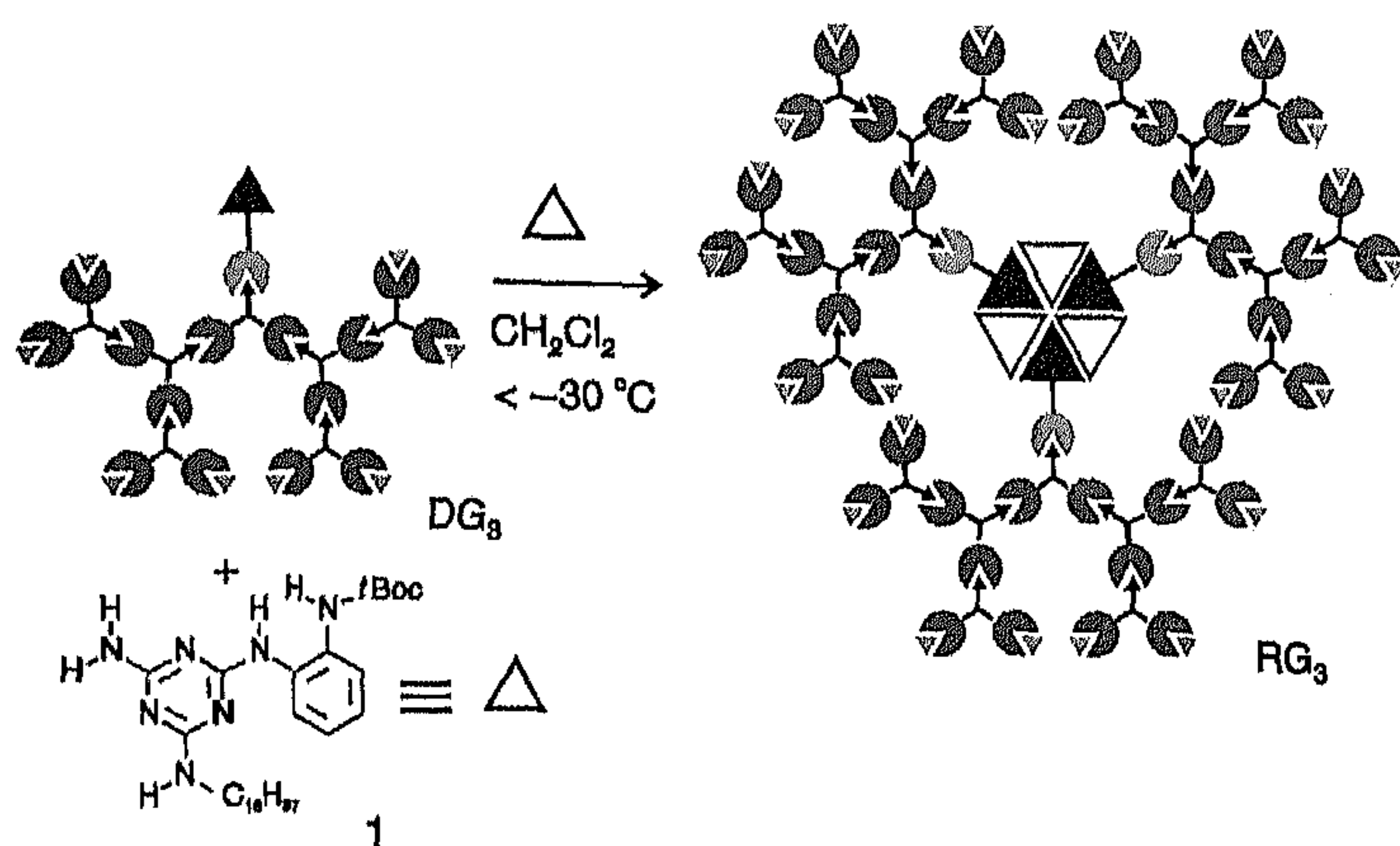
DG<sub>3</sub>: M.p. 157–158 °C; <sup>1</sup>H NMR (250 MHz, CD<sub>3</sub>NO<sub>2</sub>, 25 °C, TMS): δ = 8.56 (s, 2H, NH), 7.70–7.66 (m, 60H, Ar<sub>S</sub>H), 7.39 (s, 14H, ArH), 7.31–7.25 (m, 97H, Ar<sub>S</sub>H, ArH), 6.65 (s, 30H, Ar<sub>Pd</sub>H), 4.97 (s, 28H, CH<sub>2</sub>O), 4.5 (br. s, 60H, CH<sub>2</sub>S), 3.79 (s, 14H, CH<sub>2</sub>CN), 3.28 (s, 2H, C(O)CH<sub>2</sub>), 1.92–1.89 (m, 2H, CH<sub>2</sub>), 1.35–1.31 (m, 4H, CH<sub>2</sub>), 1.07 (t, 3H, CH<sub>3</sub>); ES-MS: *m/z* = 8625.9 ([*M* – BF<sub>4</sub> – Cl]<sup>+</sup>), calcd: 8632.7; elemental analysis calcd for C<sub>380</sub>H<sub>316</sub>O<sub>19</sub>S<sub>30</sub>N<sub>9</sub>Pd<sub>15</sub>Cl<sub>8</sub>B<sub>7</sub>F<sub>28</sub>: C 52.09, H 3.64, N 1.44, S 10.98, Cl 3.24; found: C 52.41, H 3.74, N 1.42, S 10.77, Cl 2.85.

all cases coordination of the cyano groups to the Pd centers was confirmed by FT-IR (the band for the C≡N stretch shifts from 2250 to 2290 cm<sup>–1</sup> upon coordination).<sup>[12]</sup> ES-MS spectra of solutions in CH<sub>3</sub>NO<sub>2</sub> clearly show formation of the dendrons with the masses 1765.3 Da (DG<sub>1</sub>, 1766.7 calcd for [*M* – BF<sub>4</sub>]<sup>+</sup>), 3986.0 Da (DG<sub>2</sub>, 3983.2 calcd for [*M* – 2BF<sub>4</sub>]<sup>+</sup>), and 8625.9 Da (DG<sub>3</sub>, 8632.7 calcd for [*M* – BF<sub>4</sub> – Cl]<sup>+</sup>).

The rosettes were subsequently constructed by addition of *N*-octadecan-1-yl-*N'*-(2-*N*-(Boc-amino)phenyl)melamine (1) to DG<sub>1</sub>–DG<sub>3</sub>; the assembly with DG<sub>3</sub> is depicted in Scheme 2. The barbituric acid groups bind to the melamine through six hydrogen bonds in a cyclic [3 + 3] fashion to form the hexameric rosette. Whereas DG<sub>1</sub>–DG<sub>3</sub> are only soluble in CH<sub>3</sub>NO<sub>2</sub>, the assemblies readily dissolve in CH<sub>2</sub>Cl<sub>2</sub> after addition of 1. This increased solubility is a common feature of rosettes.<sup>[13]</sup>

The structural assignment of RG<sub>1</sub>–RG<sub>3</sub> in solution (concentrations > 4 mM) is based on low temperature <sup>1</sup>H NMR (400 MHz) experiments in CD<sub>2</sub>Cl<sub>2</sub>. The characteristic signals for the rosette structure<sup>[14]</sup> are present in the range of –60 °C to –30 °C (Figure 1); they disappear at temperatures above –20 °C. Whitesides et al.<sup>[15]</sup> have shown that monoroettes are not kinetically stable on the NMR timescale. The





Scheme 2. Rosette formation of  $DG_3$  with melamine 1.

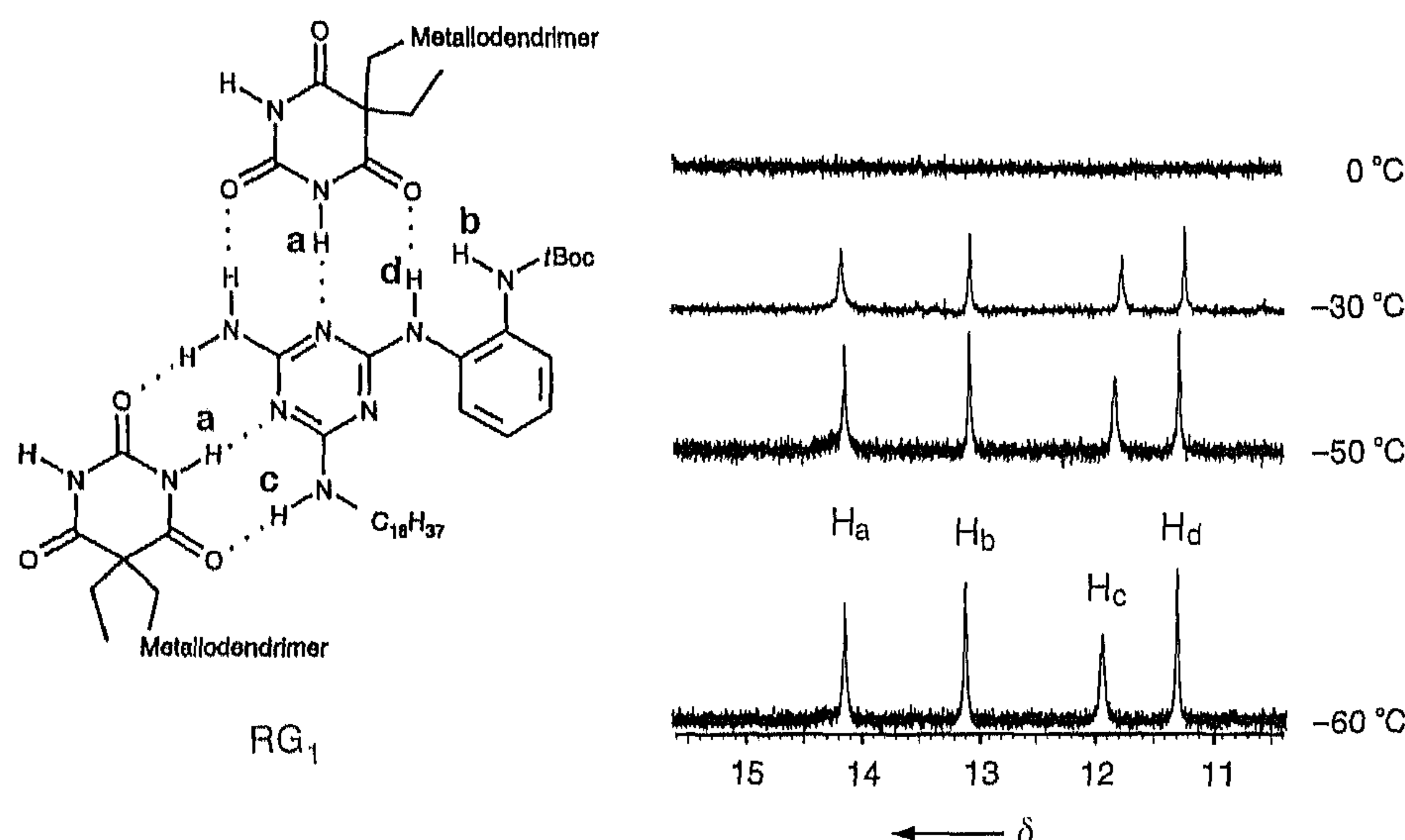


Figure 1. Low-temperature  $^1\text{H}$  NMR spectra (400 MHz) of  $RG_1$  in  $\text{CD}_2\text{Cl}_2$ .

characteristic signal at  $\delta = 14.15$  corresponds to the hydrogen-bonded imido protons of the barbituric acid residues ( $H_a$ ). Based on 2-D NOESY and TOCSY experiments, the two signals at  $\delta = 11.50$  ( $H_d$ ) and  $12.01$  ( $H_c$ ) can be assigned to the melamine NH protons. The 2-D NOESY spectrum shows strong NOE cross signals of  $H_a$  with  $H_c$  and  $H_d$  ( $\text{NH}-\text{C}_{18}\text{H}_{37}$  and  $\text{NH}-\text{phenyl}$ ) of the melamine residue. The extremely downfield-shifted signal for the  $\text{NH}-t\text{Boc}$  proton ( $H_b$ ) at  $\delta = 13.10$  does not show a NOE cross peak with  $H_a$ . Long range COSY and TOCSY experiments give further evidence that  $H_b$ ,  $H_c$ , and  $H_d$  are connected to the same fragment. The distances between the imido protons  $H_a$  and the secondary amine protons  $H_c$  and  $H_d$  were determined with the NOE initial rate approximation<sup>[16]</sup> and are in agreement with a rosette structure (Table 2).<sup>[6, 17]</sup> The gradual increase of these distances upon increasing size of the assemblies may be an indication of increasing steric interactions between the dendrons in the rosettes.

Table 2. Interatomic distances in  $RG_1$ – $RG_3$  as determined by 2-D NOESY experiments.

Rosette	$H_a-H_c$ [Å]	$H_a-H_d$ [Å]
$RG_1$	$2.5 \pm 0.1$	$2.8 \pm 0.1$
$RG_2$	$2.6 \pm 0.2$	$3.1 \pm 0.2$
$RG_3$	$2.8 \pm 0.4$	$3.4 \pm 0.4$

Rosette formation was further confirmed by build-up curves measured for the NOE interactions between the methylene bridge protons as well as other isolated resonances. This enabled us to determine the rotation correlation times  $\tau_c$ .<sup>[18]</sup> Assuming isotropic tumbling and exclusive dipole–dipole relaxation—that is, no internal motion—the cross relaxation rates  $\tau_{12}$  were determined, and the corresponding  $\tau_c$  values calculated.<sup>[19]</sup> As expected, the  $\tau_c$  values increase with increasing size of the rosette dendrimers (Table 3).<sup>[19]</sup>

Table 3. Rotation correlation times  $\tau_c$  and molecular weights.

Rosette	$\tau_c \times 10^{-9}$ [s]	$M_{\text{calcd}}$ [Da]
$RG_1$	1.32	7266
$RG_2$	2.75	14177
$RG_3$	3.55	27972

These are the first nanosized assemblies held together by two different types of noncovalent, compatible interactions: coordinative and hydrogen bonds. From a synthetic point of view it is important that the two types of interactions are "orthogonal", that is, mutually compatible. This is a prerequisite for a generally applicable methodology.

Received: November 18, 1996 [Z97921E]  
German version: *Angew. Chem.* 1997, 109, 1046–1049

**Keywords:** dendrimers • hydrogen bonds • nanostructures • NMR spectroscopy

- [1] S. C. Zimmerman, F. Zeng, D. E. C. Reichert, S. V. Kolotuchin, *Science* 1996, 271, 1095–1099.
- [2] W. T. S. Huck, F. C. J. M. van Veggel, B. L. Kropman, D. H. A. Blank, E. G. Keim, M. M. A. Smithers, D. N. Reinhoudt, *J. Am. Chem. Soc.* 1995, 117, 8293–8294.
- [3] W. T. S. Huck, F. C. J. M. van Veggel, D. N. Reinhoudt, *Angew. Chem.* 1996, 108, 1304–1306; *Angew. Chem. Int. Ed. Engl.* 1996, 35, 1213–1215.
- [4] Examples of infinite networks: M. M. Chowdry, D. M. P. Mingos, A. J. P. Smith, D. J. Williams, *Chem. Commun.* 1996, 899–900; A. D. Burrows, C.-W. Chan, M. M. Chowdry, J. E. McGrady, M. D. P. Mingos, *Chem. Soc. Rev.* 1995, 331–339.
- [5] G. M. Whitesides, E. E. Simanek, J. P. Mathias, C. T. Seto, D. N. Chin, M. Mammen, D. M. Gordon, *Acc. Chem. Res.* 1995, 28, 37–44.
- [6] R. H. Vreekamp, J. P. M. van Duynhoven, M. Hubert, W. Verboom, D. N. Reinhoudt, *Angew. Chem.* 1996, 108, 1306–1309; *Angew. Chem. Int. Ed. Engl.* 1996, 35, 1215–1218.
- [7] D. A. Tomalia, A. M. Naylor, W. A. Goddard III, *Angew. Chem.* 1990, 102, 119–157; *Angew. Chem. Int. Ed. Engl.* 1990, 29, 138–175.
- [8] C. J. Hawker, J. M. J. Fréchet, *J. Am. Chem. Soc.* 1990, 112, 7638–7642.
- [9] Synthesis of  $DG_0$ : 5-(1-butyl)-5-(2-hydroxycarbonylmethyl)barbituric acid [10] was coupled through the acid chloride to 3,5-bis(phenylthiomethyl)phenol and isolated in 33% yield after purification. Subsequent cyclopalladation with  $[\text{Pd}(\text{CH}_3\text{CN})_4](\text{BF}_4)_2$ , stirring with brine, and purification by column chromatography ( $\text{SiO}_2$ ,  $\text{CH}_2\text{Cl}_2/\text{MeOH}$  95/5) gave  $DG_0$ .
- [10] P. Tecilla, V. Jubian, A. D. Hamilton, *Tetrahedron* 1995, 51, 435–448.
- [11] B. N. Storhoff, H. C. Lewis, *Coord. Chem. Rev.* 1977, 23, 1–23.
- [12] J. P. Mathias, E. E. Simanek, G. M. Whitesides, *J. Am. Chem. Soc.* 1994, 116, 4326–4340.
- [13] C. T. Seto, J. P. Mathias, G. M. Whitesides, *J. Am. Chem. Soc.* 1993, 115, 1321–1329.
- [14] J. P. Mathias, E. E. Simanek, J. A. Zerkowski, C. T. Seto, G. M. Whitesides, *J. Am. Chem. Soc.* 1994, 116, 4316–4325.
- [15] R. R. Ernst, G. Bodenhausen, A. Wokaun in *Principles of Nuclear Magnetic Resonance in One and Two Dimensions*, Vol. 14 (Eds.: R. Breslow, J. B. Goodenough, J. Halpern, E. Rowlinson), Clarendon, Oxford, 1987, p. 490.



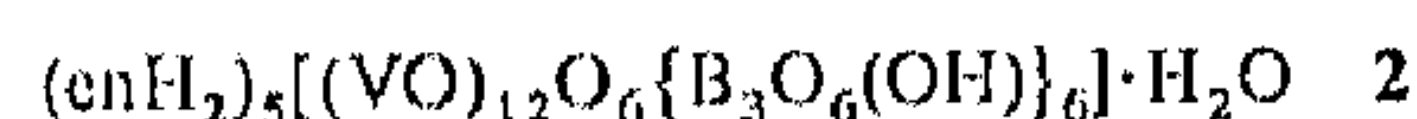
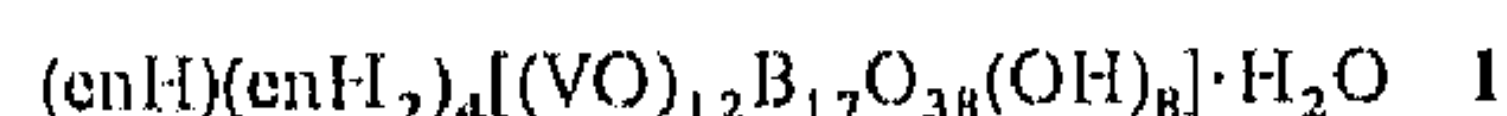
- [16] Data obtained for RG<sub>3</sub> shows a larger error due to the large size of the molecule.
- [17] K. Wütrich, *NMR of Proteins and Nucleic Acids*, Wiley, New York, 1986, chap. 6.
- [18] For a two-spin system with atoms 1 and 2, the cross relaxation constant  $\tau_{12}$  and rotation correlation time  $\tau_c$  are related as in Equation (1). Isotropic tumbling
- $$\tau_{1/2} = 1/10(\mu_0/2\pi)^2([\gamma_1^4(h/2\pi)^2]/r^6(\tau_c/(1 + 4\omega^2\tau_c^2) - \tau_c)) \quad (1)$$
- and pure dipole-dipole relaxation are assumed.  $\mu_0$  = dielectric constant,  $\gamma$  = gyromagnetic constant,  $r$  = distance between atoms 1 and 2, and  $\omega$  = Larmor frequency. Measurements were conducted with a 400 MHz instrument.
- [19] T. L. James, G. B. Matson, I. D. Kuntz, *J. Am. Chem. Soc.* **1978**, *100*, 3590–3594.

## Novel Clusters of Transition Metals and Main Group Oxides in the Alkylamine/Oxovanadium/Borate System

Job T. Rijssenbeek, David J. Rose, Robert C. Haushalter,\* and Jon Zubieta\*

*Dedicated to Professor Hans Georg von Schnering on the occasion of his 66th birthday*

Hydrothermal synthesis is an area of rapidly increasing importance for the synthesis of new and structurally complex, hybrid, organic-inorganic, solid-state compounds. Utilizing the ability of polar organic molecules to direct the crystallization of inorganic frameworks by incorporation in a geometrically specific manner through multipoint hydrogen bonding, we have been able to prepare several new classes of materials. Pre-synthesized organic molecules were used to imprint structural information onto inorganic oxide lattices, and microporous solids with the largest cavities and lowest framework densities known,<sup>[1]</sup> lamellar transition metal oxides or phosphates with organic cations<sup>[2]</sup> or coordination compounds<sup>[3]</sup> between the layers, polyoxometalates linked by coordination compounds into 2-D and 3-D solids,<sup>[4]</sup> materials with interlaced 1-D organic and inorganic chains,<sup>[5]</sup> and organically templated transition metal halides<sup>[6]</sup> have all been made. Even polyoxometalate metal species,<sup>[7]</sup> including the unusual  $[\text{H}_{16}(\text{VO}_2)_{16}(\text{CH}_3\text{PO}_3)_8]^{8-}$ ,<sup>[8]</sup> have been synthesized by hydrothermal synthesis. We report here the use of this technique for the synthesis of **1** and **2** (en = ethylenediamine), which represent a novel type



[\*] Dr. R. C. Haushalter, J. T. Rijssenbeek  
NEC Research Institute  
4 Independence Way  
Princeton, NJ 08540 (USA)  
Fax: Int. code + (609) 951-2483  
Prof. J. Zubieta, D. J. Rose  
Department of Chemistry  
Syracuse University  
Syracuse, NY 13244 (USA)  
Fax: Int. code + (315) 443-4070  
e-mail: jazubiet@mailbox.syr.edu

[\*\*] The work at Syracuse University was supported by the U. S. National Science Foundation (grant no. 9318824).

of clusters of transition metals and main group oxides in the organic cation/vanadium/borate system and possess unprecedented structures. Although a large number of borate mineral structures are known,<sup>[9]</sup> and substantial progress has been made in classifying and understanding their structures, synthetically prepared and structurally characterized examples are rare.<sup>[10, 11]</sup>

The general procedure for preparing **1** and **2**, as well as other vanadium borate clusters,<sup>[12]</sup> consists of concentrated hydrothermal treatment of a vanadium oxide source ( $\text{V}_2\text{O}_3$  or  $\text{V}_2\text{O}_5$ ) with  $\text{B}_2\text{O}_3$  or  $\text{H}_3\text{BO}_3$  and amine at 170 °C in water. Large, structurally complicated, highly crystalline clusters spontaneously form in good yield from these simple starting materials and synthetic conditions.

The structure of the  $\text{V}_{12}\text{B}_{17}$  cluster in **1**<sup>[13]</sup> contains several highly interesting features, the most extraordinary of which may be the contorted vanadium oxide ring (Figure 1a). The ring can be described as two semicircles of five *trans*, edge-sharing  $\text{VO}_5$  square pyramids that partially interpenetrate—like the seams on a tennis ball. The four ends of the semicircles connect through two additional  $\text{VO}_5$  units to form a continuous  $\text{V}_{12}$  ring of unprecedented connectivity (Figure 1b). All 12 terminal vanadyl ( $\text{V}=\text{O}$ ) groups radiate away from the cluster surface. The clefts formed by the ring are occupied by two novel  $\text{B}_8$  and  $\text{B}_9$  polyborate chains (Figure 1c). The  $\text{B}_8\text{O}_{17}(\text{OH})_4$  chain is composed of two linked  $\text{B}_3\text{O}_6(\text{OH})$  FBBs (fundamental building blocks)<sup>[17]</sup> that are capped on each end by a tetrahedral  $\text{BO}_3(\text{OH})$  group. The second chain,  $\text{B}_9\text{O}_{18}(\text{OH})_4(\text{enH})$ , retains the approximate shape of the first. However, the OH groups on the terminal boron atoms have been replaced by a pendant, planar  $\text{BO}(\text{OH})_2$  triangle on one end and an  $\text{enH}^+$  molecule on the other to give a tetrahedral  $\text{BO}_3\text{N}$  coordination environment (Figure 1a). The interior cavity of the cluster is occupied by poorly defined electron density, probably due to an occluded  $\text{H}_2\text{O}$  molecule. The intercluster space is filled by  $\text{enH}_2^{2+}$  and water molecules.

The  $\text{V}_{12}\text{B}_{18}$  cluster in **2**<sup>[14]</sup> consists of a puckered  $\text{B}_{18}\text{O}_{36}(\text{OH})_6$  ring sandwiched between two triangles of six alternating *cis* and *trans*, edge-sharing vanadium atoms. Each vertex of this novel triangular metal-oxo moiety contains a *cis*, edge-sharing  $\text{VO}_5$  square pyramid, whereas the midpoint of each edge is occupied by a *trans*, edge-sharing  $\text{VO}_5$  polyhedron (Figure 2a–c). Again, all the vanadyl groups radiate away from the cluster surface. The  $\text{B}_{18}$  ring (Figure 2d,e) is composed of six  $\text{B}_3\text{O}_6(\text{OH})_4^-$  FBBs and exists in a cyclohexane-like chair conformation with a  $\text{B}_3$  unit at each of the six vertices. The two  $\text{V}_6$  triangles are coordinated to each face of the  $\text{B}_{18}$  ring through six “axial” B–O–V bonds and three  $\text{B}_2-(\mu_3\text{-O})\text{-V}$  bonds. On average, ten of the twelve vanadium atoms per cluster are  $\text{V}^{\text{IV}}$ , and two are  $\text{V}^{\text{V}}$ ; this accounts for the dark red color of the crystals. The V oxidation states were determined by considering the other known charges present in the unit cell and confirmed by valence bond calculations,<sup>[15]</sup> which show a valence of about +4.22 for each V atom. This value is close to the +4.17 expected for a  $\text{V}^{\text{IV}}:\text{V}^{\text{V}}$  ratio of 5:1, and it appears that each vanadium site has an equal possibility of containing a  $\text{V}^{5+}$  ion.

Consistent with the fact that borate minerals are often found in dry lakebeds,<sup>[16]</sup> the borate starting material remains in solution if too much water is present during the synthesis of these oxovanadium borates, and single crystals of layered vanadium oxides<sup>[2]</sup> are formed. We have observed, in this and other hydrothermal metal oxide systems, that the presence of a small amount of dissolved borate (from  $\text{B}_2\text{O}_3$  or  $\text{H}_3\text{BO}_3$ ) greatly enhances the dissolution of the starting materials and very favorably affects the subsequent crystallization of the metal oxide.